Green and Direct Synthesis of Benzaldehyde and Benzyl Benzoate in One Pot

Mina Ghahremani,[‡,†] Rosaria Ciriminna,[†] Valerica Pandarus,[§] Antonino Scurria,[†] Valeria La Parola,[†] Francesco Giordano,[†] Giuseppe Avellone,[||] Francois Béland,*[,§] Babak Karimi,*[,‡] and Mario Pagliaro*[,†]

[†]Istituto per lo Studio dei Materiali Nanostrutturati, CNR via U. La Malfa 153, 90146 Palermo, Italy
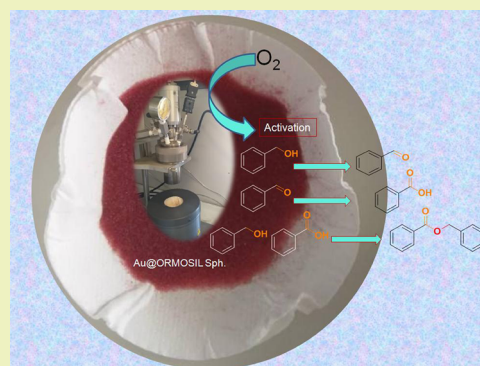
[‡]Institute for Advanced Studies in Basic Sciences, No. 444, Prof. Yousef Sobouti Boulevard, P.O. Box 45195-1159, Zanjan, Iran

[§]SiliCycle, 2500 Parc-Technologique Boulevard, Québec, Québec G1P 4S6, Canada

[||]Dipartimento di Scienze e Tecnologie Biologiche Chimiche e Farmaceutiche, Università degli Studi di Palermo, via Archirafi 32, 90123 Palermo, Italy

S *Supporting Information*

ABSTRACT: High yields of valued benzaldehyde and benzyl benzoate are obtained in one pot starting from benzyl alcohol using oxygen as only oxidant under mild conditions (2 bar O_2, 100 °C) along with an ultralow amount (0.02 mol %) of Au nanoparticles heterogenized over a spherical ORMOSIL mesoporous support. The process is remarkably selective and the catalyst is stable.

INTRODUCTION

Nowadays successfully employed in the commercial synthesis of vinyl chloride monomer via hydrochlorination of acetylene in China (where it replaces toxic mercury chloride supported on carbon),[1] supported gold nanoparticles (NPs) are exceptional catalytic species with a truly broad scope of application, including clean oxidation and hydrogenation reactions with O_2 and H_2 in liquid phase.[2] Gold-mediated selective oxidation of alcohols using O_2 or H_2O_2 as primary oxidants is among the synthetic transformations whose uptake by the fine chemical and pharmaceutical industries is likely to occur shortly.[3] Of particular interest are solvent-free catalytic processes with no waste generation via selective and efficient solid catalysts of pronounced stability,[4] suitable to be carried out under flow.[5]

In general, the catalytic activity of Au supported nanoparticles is affected mainly by the nature of the support, which dictates the fundamentally important Au-support interface interaction[2] and by the size of Au NPs, which in turn depends on the synthetic methodology affording the catalytic material. Loading electron-rich Au nanocrystallites on reducible supports promotes the adsorption and activation of O_2;[6] whereas Tata and co-workers, reporting the much higher activity of Au/SrTiO$_3$ compared to Au/TiO$_2$ for the alcohol oxidation and H_2O_2 decomposition, lately suggested that the

rate-determining step in these oxidative reactions is the electron transfer from Au NP to O_2 and H_2O_2.[7]

Similarly, relatively large Au NPs (with a diameter of 14.4−52 nm) sol−gel encapsulated within the inner mesopores of 5% methyl-modified silica, selectively mediate the solvent-free oxidation of several alcohols under mild conditions (100 °C, 2 bar O_2) in the presence of carbonate as promoter;[8] as well as the oxidation of secondary alcohol using Cao's biphasic protocol with H_2O_2.[9] Now, we show how the reactivity of Au nanoparticles xerogels can be further enhanced by depositing the gold NPs in fully alkylated silica xerogel of spherical morphology.

RESULTS AND DISCUSSION

In detail, the Au nanoparticles were deposited by impregnation-deposition within the inner mesoporosity of spherical 100% methyl-modified silica (Sph. ORMOSIL) and irregular (nonspherical) silica (NSp.Silica) through colloidal deposition and the catalytic activity of the resulting catalytic materials assessed in the solvent-free oxidation aerobic of benzyl alcohol.

Table 1 and Figure 1 (in which isotherms are shifted along the y-axis for clarity) illustrate the textural properties of both

Table 1. Textural Properties of Nonspherical Silica and Spherical ORMOSIL and the Corresponding Gold Catalysts

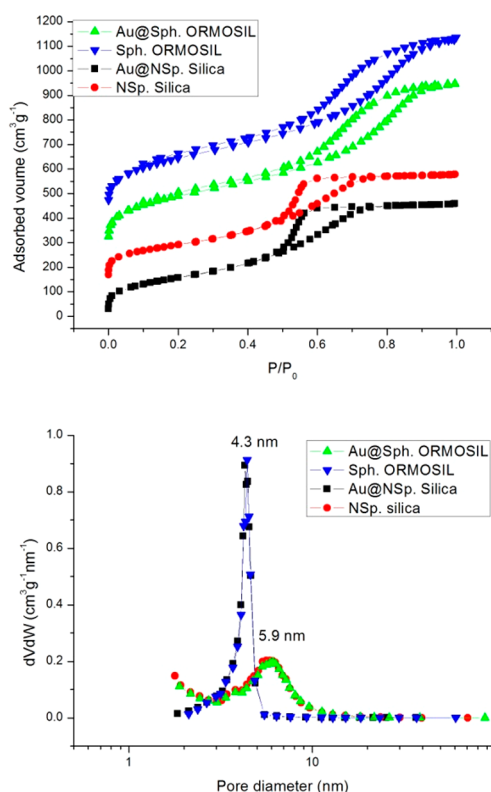| Material	SSA (m^2 g^{-1})	V_P (cm^3 g^{-1})
NSp silica	519	0.68
Au@NSp silica	579	0.73
Sph.ORMOSIL	736	1.03
Au@Sph.ORMOSIL	679	1.05

Figure 1. N$_2$ adsorption–desorption isotherms of NSp.Silica and Sph.ORMOSIL blank materials and the corresponding gold catalysts (top), and pore size distribution (bottom).

NSp silica and Sph.ORMOSIL and the corresponding gold catalysts. The N$_2$ adsorption–desorption isotherms are of type IV with hysteresis loops characteristic of mesoporous materials. According to the IUPAC classification, the hysteresis loops of the NSp silica and Sph.ORMOSIL can be classified as H1 and H3 types, respectively. The hysteresis loop of NSp and Au@NSp.Silica are larger and typically of the presence of mesopores.[10] In contrast, the hysteresis loops of the Sph.ORMOSIL support and of Au@Sph.ORMOSIL catalyst were rather flat and extended over a large range of relative pressures, indicating the presence of both framework mesoporosity and interparticle macroporosity.[10]

The spherical ORMOSIL materials are characterized by higher surface area and pore specific volume, compared to the nonspherical silica-based materials. The slight decrease of the surface area (from 736 to 679 m^2 g^{-1}) and almost unvaried pore volume (from 1.03 to 1.05 cm^3 g^{-1}, Table 1) of the spherical ORMOSIL upon deposition of the Au nanoparticles by impregnation-deposition indicates that the Au nanoparticles are located at the external surface of the inner porosity typical

of sol−gel hybrid glasses, with no pore obstruction. On the contrary the nonspherical Au@NSp.Silica material shows a higher surface area and pore volume with respect to the corresponding support indicating a contribution of the gold particles to the total surface area.

Figure 2 shows the presence of Au nanoparticles revealed by X-ray diffraction in all catalyst samples. The diffractions peaks
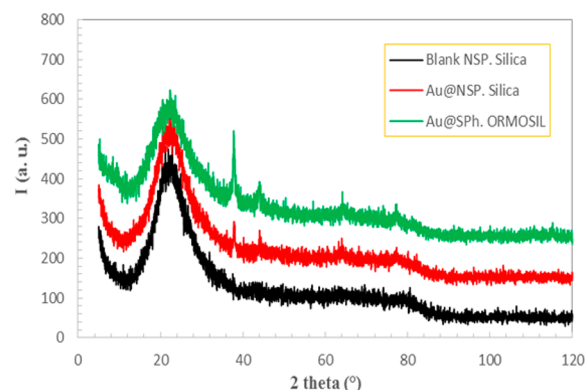

Figure 2. XRD spectrum of Au@SPh.ORMOSIL, Au@Nsp.Silica, and blank nonspherical silica.

from the (111), (200), (220) and (311) Au crystal facets indicates the crystalline nature of the gold nanoparticles.[11] The higher and diffraction peaks in the spherical (green line) material when compared to the nonspherical silica-based material (red line) point to more ordered Au nanoparticles entrapped in the spherical support. The spherical catalyst incorporates Au nanoparticles 23 nm in size whereas the nonspherical material embeds NPs with average 29 nm diameter. Gold nanoparticles exhibit a considerable local structural disorder that diminishes with their size, with models based on a fragment of a locally disordered fcc-type lattice providing a good description of the 3-D structure of 15 and 30 nm nanoparticles.[11]

The X-ray photoelectron spectroscopy survey of Au@Sph.ORMOSIL in Figure 3 (representative of all samples) confirms the presence of C, Si, O and Au as the only elements comprising these materials.

The analysis of the high resolution region of Au 4f emission shows the typical two spin−orbit components, Au 4f$_{7/2}$ and Au 4f$_{5/2}$, with a separation of 3.6 eV and ratio area of Au 4f$_{7/2}$/Au 4f$_{5/2}$ of 1.5. The deconvolution of the Au 4f$_{7/2}$ peak, shown in Figure 4, indicates the presence of metallic gold for Au@Nsp.Silica (BE= 83.9 eV), whereas for Au@Sph.ORMOSIL
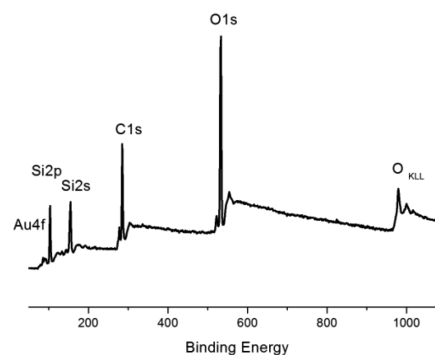

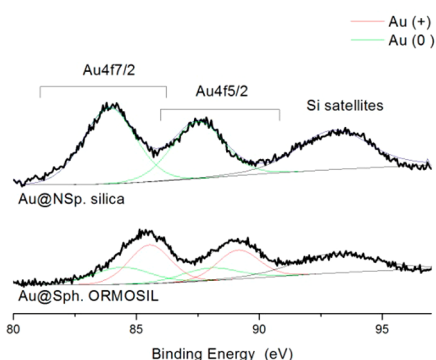**Figure 3.** XPS survey spectrum of Au@Sph.ORMOSIL.

Figure 4. XPS high resolution Au 4f region of Au@NSp.Silica and Au@Sph.ORMOSIL.

gold is present as both metallic gold Au^0 (BE 84.1−84.3 eV) and cationic gold Au^{1+} (BE = 85.5−85.8 eV).[12] The relative percentage of the two gold species expressed as a percentage of the total area of the Au 4f peak (taken as 100%) is given in Table 2 along with Au/Si and C/Si ratio.

Table 2. Au $4f_{7/2}$ Binding Energy, Au/Si and C/Si Atomic Ratio, and Relative Percentage of Au^0 and Au^{+1} in Nonspherical Silica and Spherical ORMOSIL Gold Catalysts

Material	Au $4f_{7/2}$ BE (eV)	Au surface species	Au/Si	C/Si
Sph.ORMOSIL				1.2
Au@Sph.ORMOSIL	84.4	Au^0 (38%)	0.013	1.5
	85.5	Au^{1+} (62%)		
Au@NSp.Silica	83.9	Au^0 (100%)	0.011	

The Au/Si ratios are quite similar for all the samples indicating an analogous dispersion and particles size, confirming the outcomes of the XRD analyses. An increase of the C/Si ratio for Au catalysts deposited on the spherical support samples with respect to the bare (blank) support shows that Au nanoparticles are located mainly on top of silicon atoms, more than on the Si-bound methyl groups.

Transmission electron microscopy investigation of Au@Sph.ORMOSIL and Au@NSp.Silica (Figure 5) confirms the indirect findings of the BET analysis, with the Au nanoparticles clearly visible on the glassy structure of silica-based material, but trapped inside and not revealed by electron microscopy for the spherical ORMOSIL catalyst, with the matrix mesoporosity clearly visible for both sol−gel glasses.

Tested in the solvent-free aerobic oxidation of benzyl alcohol affording benzaldehyde under relatively mild conditions (2 bar O_2, 100 °C), the spherical organosilica catalyst Au@Sph.ORMOSIL was considerably more active than the nonspherical silica-based material Au@Nsp.Silica, as well as of the irregular 5% methyl-modified SiliaCat Au organosilica catalyst.

In detail, after 20 h the reaction over the spherical ORMOSIL affords 38% substrate conversion (entry 2 in Table 3), followed by 25% over the nonspherical material (entry 3), and 10% over SiliaCat Au (entry 1 in Table 3). The conversion of benzyl alcohol over Au@NSp. Silica was >2 times higher than with SiliaCat Au (10%), but the selectivity to aldehyde decreased to 60% (entry 3) with 40% selectivity to benzyl benzoate.
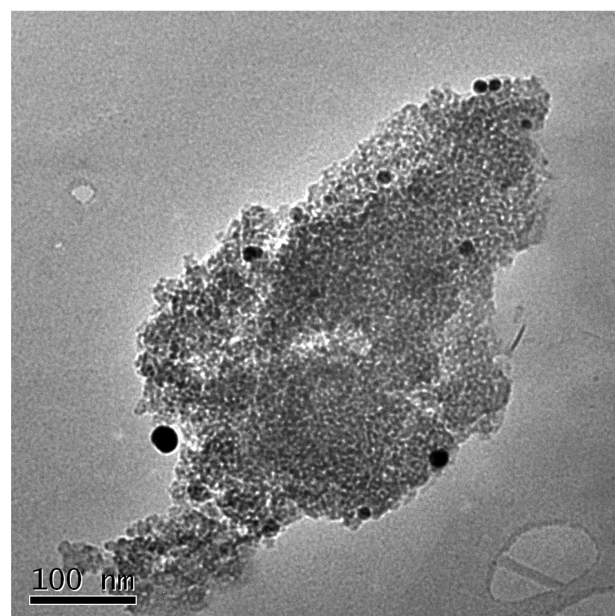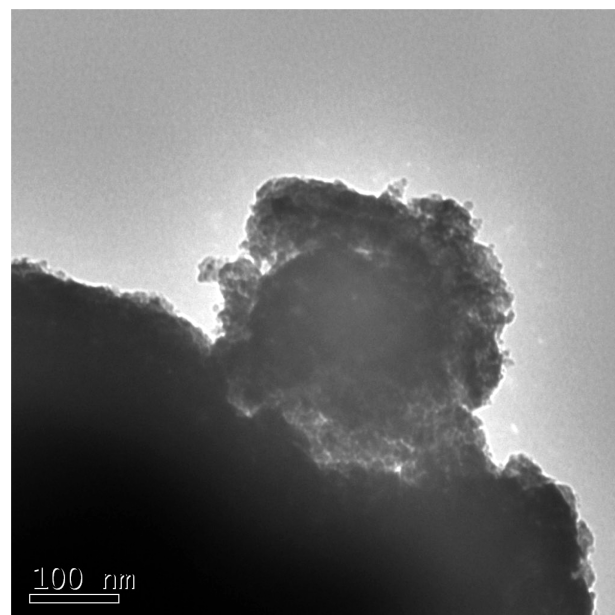

Figure 5. TEM micrographs of Au@SPh.ORMOSIL (top, 2500×) and Au@NSp.Silica (bottom, 3000×).
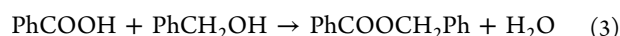
Table 3. Aerobic Oxidation of Benzy Alcohol over Different Sol−Gel Catalysts Functionalized with Au Nanoparticles[a]

Entry	Catalyst	Alcohol conversion (%)	Benzaldehyde yield (%)	Benzyl benzoate yield (%)
1	SiliaCat Au	10	9.4	−
2	Au@Sph.ORMOSIL	38	25	13
3	Au@NSp.Silica	25	15	10

[a]Reaction conditions: 10 mL benzyl alcohol, 0.02 mol % Au, K_2CO_3 1 mol %, 100 °C, 2 bar O_2, under stirring; conversion and selectivity to aldehyde via GC analysis after 20 h reaction time.

The latter 5% methyl-modified silica functionalized with Au NPs confirmed its high selectivity toward aldehyde formation via direct catalytic oxidative dehydrogenation of benzyl alcohol

yielding benzaldehyde with 94% selectivity (eq 1). The spherical catalyst affords the highest substrate conversion with 66% selectivity to benzaldehyde (25% yield at 38% conversion), and 34% selectivity to benzyl benzoate formed in high 13% yield via the esterification of benzoic acid formed upon further oxidation of the aldehyde (eq 2) reacting with the alcohol substrate (eq 3).

$$PhCH_2OH + \frac{1}{2}O_2 \rightarrow PhCHO + H_2O \tag{1}$$

$$PhCHO + \frac{1}{2}O_2 \rightarrow PhCOOH \tag{2}$$

$$PhCOOH + PhCH_2OH \rightarrow PhCOOCH_2Ph + H_2O \tag{3}$$

Remarkably, contrary to what happens with Au nanoparticles deposited over titania[13] or over zeolites[14] employed in the same solvent-free aerobic oxidation of benzyl alcohol, no toluene formed via disproportionation of benzyl alcohol into benzaldehyde, toluene and water ($2PhCH_2OH \rightarrow PhCHO + PhCH_3 + H_2O$) was observed.

The spherical ORMOSIL catalyst and the irregular Au@NSp.Silica xerogel were therefore tested for stability in 6 consecutive reaction runs. After reaction, the catalytic material was filtered, washed with EtOAc, deionized water and dried at 80 °C and reused in a subsequent run. To our delight, the spherical Au@Sph.ORMOSIL catalyst was found to be largely recyclable (green bars in Figure 6). On the other hand, Au@NSp.Silica lost two-thirds of its activity after three reaction runs.
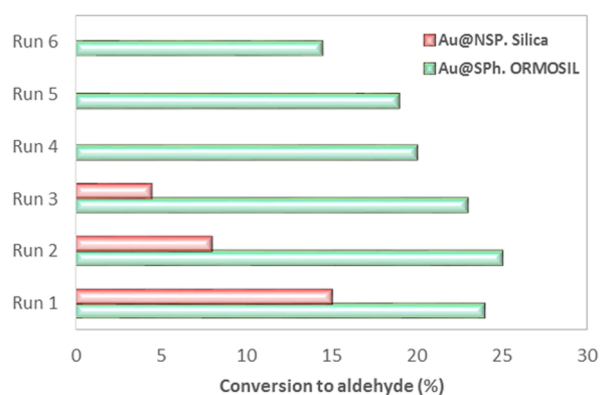

Figure 6. Reusability of Au@Sph.ORMOSIL and Au@NSP.Silica. Reaction conditions: 10 mL benzyl alcohol, 0.02 mol % Au, 100 °C, K_2CO_3 1 mol %, 2 bar O_2, under stirring.

In general, noble metal nanoparticles sol−gel entrapped within ORMOSIL irregular ceramic microparticles are considerably less susceptible to leaching, as compared to other types of support.[15] Here, furthermore, the deposition of preformed Au nanoparticles onto spherical microparticles composed of fully methylated hydrophobic ORMOSIL matrix is highly advantageous because it enables the deposition of mostly positively charged Au^+ species that are stabilized by the electron donating −CH_3 groups at the ORMOSIL surface, and dramatically enhances diffusion of the reactant benzyl alcohol and O_2 molecules to the Au nanoparticles, as in the case of catalytic hydrogenolysis of C−O bonds mediated by similar spherical catalytic ORMOSIL embedding Pd nanoparticles.[16]

Previous XPS investigation of the 5% methylated xerogel catalyst doped with Au nanoparticles revealed a very feeble Au

4f photoelectronsignal.[17] Now, the straightforward deposition-precipitation method applied to a as-synthesized ORMOSIL spherical matrix affords a catalyst in which Au^0 and Au^{1+} species are clearly detected by XPS on the surface of a catalyst suitable to selectively convert benzyl alcohol into valued benzaldehyde and benzyl benzoate.

Extensive structural investigation of fully methylated ORMOSIL xerogels has shown that the surface of these materials is devoid of silanol groups.[18] Hence, no competing reactions catalyzed by the acid-basic sites of the catalyst surface take place as it happens, for instance, when Au nanoparticles are deposited at the surface of zeolites.[14] Acting as an hydrophobic chemical sponge,[19] furthermore, the ORMOSIL surface promotes the esterification reaction (eq 3), and consequent water loss.

■ CONCLUSION

These findings are important because both benzaldehyde and benzyl benzoate are valued industrial products. Generally regarded as safe (GRAS) by the U.S. Food and Drug Administration, benzaldehyde is used as a flavoring and fragrance agent added directly in perfumes, soaps, foods, drinks, cosmetics and pharmaceuticals.[20] So far industrially produced via the hydrolysis of benzal chloride or the partial oxidation of toluene, benzaldehyde is also an important starting material for the production of odorants and flavors, whose gas-phase synthesis at 203 °C from benzyl alcohol in 99% yield over Cu(I) heterogenized over mesoporous titania, was reported by Stucky, Fan and co-workers in 2009.[21]

Benzyl benzoate, in its turn, is a potent acaricide listed in the World Health Organization's list of the most important medications needed in basic health systems,[22] being commonly used for treatment of scabies infectious skin disease as well of pediculosis. Industrially synthesized via esterification reaction of sodium benzoate with benzyl alcohol, it is also as textile auxiliary, fragrance solvent (the only solvent of musk) and plasticizer in high demand, whose direct synthesis from toluene in a solvent-free process over Au−Pd nanoparticles supported on carbon was reported by Hutchings and co-workers in 2011.[23]

The results of this study show that it is enough the carry out the oxidative dehydrogenation reaction of benzyl alcohol over a stable spherical gold catalyst to obtain high yields of both products under solvent-free conditions which are ideal from the green chemistry viewpoint (principle #1 of green chemistry: prevention of waste).[24] Since mesoporous ORMO-SIL catalysts, are ideally suited for reactions under flow,[25] higher conversion and yields are expected by prolonging the reaction time and by transferring the reaction from batch to flow conditions.

■ EXPERIMENTAL SECTION

Silia*Cat* Au was prepared by sol−gel entrapment of Au^{3+} stabilized by poly(vinyl alcohol) followed by reduction with $NaBH_3CN$ and calcination at 250 °C as previously reported[9] To prepare the two new catalysts, a colloidal solution of Au NPs was first prepared by treating a (Au/Support = 1 wt %) solution of $HAuCl_4$ with a 5 molar excess of $NaBH_3CN$ (0.1 M) dissolved in water containing poly(vinyl alcohol) (PVA) (1 wt %, Aldrich, MW = 10^4, 80% hydrolyzed; PVA:Au (w/w) = 1.2). The spherical ORMOSIL catalyst Au@Sph. was prepared by treating 5 g of fully alkylated ORMOSIL spherical material obtained starting from methyltriethoxysilane only (prepared at SiliCycle) with a colloidal solution of Au NPs stabilized with PVA kept under vigorous stirring (1400 min^{-1}) followed by careful adjustment of the solution

acidity to pH = 1 with H_2SO_4 (1 M). The resulting mixture was left under stirring for 2 h, after which the solid thereby obtained was separated, extensively washed with deionized water and dried overnight at 120 °C followed by calcination for 3 h at 250 °C under air using a heating rate 5 °C min^{-1}.

The nonspherical catalyst Au@NSP.Silica was prepared in two step. First, the nonspherical blank material was synthesized by the sol−gel hydrolytic polycondensation of tetraethoxysilane (TEOS) according a previously reported procedure.[15] The Au NPs were thus deposited using the same deposition-precipitation method starting from $HAuCl_4$ employed for the Au@Sph.ORMOSIL preparation.

The solvent-free aerobic oxidation of benzyl alcohol (100 mmol, 10 mL) was carried out each time in a Parr benchtop batch steel reactor equipped with 4842 Temperature Controller (Parr Instrument Company, Moline, IL) kept in a fumehood. The reaction temperature controlled by a thermostat was set at 100 °C under an initial O_2 pressure of 2 bar in the presence of the gold catalyst (0.02% mol Au) and K_2CO_3 (1 mol %). The mixture was kept under stirring for 20 h, after which the reactor was opened and the mixture content analyzed using A Shimadzu GC-17 gas chromatograph equipped with a GC capillary column Supelco (SPB-1701, matrix active phase: poly(14% cyanopropylphenyl/86% dimethylsiloxane)) and a FID detector.

The yield and conversion in benzaldehyde and benzyl benzoate were assessed via the internal standard method using previously recorded standard curves. The presence of benzyl benzoate was confirmed via mass spectrometry after separation of the ester from the reaction mixture over a silica column. An aliquot (10 μL) of the product dissolved in ethyl acetate was injected in a Thermo Fisher GC−MS (TRACE 1310 GC and TSQ 8000 MS) spectrometer using a capillary column (BPX5). Only benzyl benzoate was detected (Figure S1).

The X-ray photoelectron spectroscopy (XPS) analyses were performed with a VG Microtech ESCA 3000 Multilab, equipped with a dual Mg/Al anode. As excitation source was used the unmonochromatized Al Kα radiation (1486.6 eV). The sample powders were analyzed mounted on a double-sided adhesive carbon tape. The pressure in the analysis chamber was in the range of 10−8 Torr during data collection. The constant charging of the samples was removed by referencing all the energies to the Si 2p set at 103.5 eV, as internal standard. Analyses of the peaks were performed with the software CasaXPS. Atomic concentrations were calculated from peak intensity using the sensitivity factors provided with the software. The binding energy values are quoted with a precision of ±0.15 eV and the atomic percentage with a precision of ±10%.

The textural characterization was performed with a Micromeritics ASAP 2020 Plus instrument. The fully computerized analysis of the nitrogen adsorption isotherm at 77 K allowed to estimate the specific surface areas of the samples, through the BET method in the standard pressure range 0.05−0.3 P/P_o. By analysis of the desorption curve, using the BJH calculation method, the pore size distribution was also obtained. The total pore volume (V_p) was evaluated on the basis of the amount of nitrogen adsorbed at a relative pressure of about 0.98.

The high resolution-transmission electron micrographs were acquired with a JEOL JEM-2100 transmission electron microscope operating at 200 kV accelerating voltage. A few milligrams of each sample was suspended in 1 mL of deionized water. A drop of each suspension was placed onto a copper holey carbon coated grid and dried overnight prior TEM analysis. Micrographs were analyzed by Gatan (USA) Digital Micrograph software.

■ ASSOCIATED CONTENT

Ⓢ Supporting Information

The Supporting Information is available free of charge on the ACS Publications website at DOI: 10.1021/acssusche-meng.8b03893.

GC−MS analysis details for benzyl benzoate reaction product (PDF)

■ AUTHOR INFORMATION

Corresponding Authors
*M. Pagliaro. E-mail: mario.pagliaro@cnr.it.
*Prof. B. Karimi. E-mail: karimi@iasbs.ac.ir.
*Dr. F. Béland. E-mail: FrancoisBeland@silicycle.com.

ORCID ⊙
Valeria La Parola: 0000-0001-7695-6031
Mario Pagliaro: 0000-0002-5096-329X

Notes
The authors declare no competing financial interest.

■ REFERENCES

(1) Johnston, P.; Carthey, N.; Hutchings, G. J. Discovery, Development, and Commercialization of Gold Catalysts for Acetylene Hydrochlorination. *J. Am. Chem. Soc.* **2015**, *137*, 14548−14557.

(2) Ishida, T.; Haruta, M. Supported Gold Nanoparticles Leading to Green Chemistry In *Nanotechnology in Catalysis: Applications in the Chemical Industry, Energy Development, and Environment Protection*; van de Voorde, M., Sels, B., Eds.; Wiley-VCH: Weinheim, 2017; pp 21−36.

(3) Sharma, A. S.; Kaur, H.; Shah, D. Selective oxidation of alcohols by supported gold nanoparticles: recent advances. *RSC Adv.* **2016**, *6*, 28688−28727.

(4) Ni, J.; Yu, W.-J.; He, L.; Sun, H.; Cao, Y.; He, H.-Y.; Fan, K.-N. A Green and Efficient Oxidation of Alcohols by Supported Gold Catalysts Using Aqueous H_2O_2 Under Organic Solvent-Free Conditions. *Green Chem.* **2009**, *11*, 756−759.

(5) Constantinou, A.; Wu, G.; Corredera, A.; Ellis, P.; Bethell, D.; Hutchings, G. J.; Kuhn, S.; Gavriilidis, A. Continuous Heterogeneously Catalyzed Oxidation of Benzyl Alcohol in a Ceramic Membrane Packed-Bed Reactor. *Org. Process Res. Dev.* **2015**, *19*, 1973−1979.

(6) Della Pina, C.; Falletta, E.; Rossi, M. Update on Selective Oxidation Using Gold. *Chem. Soc. Rev.* **2012**, *41*, 350−369.

(7) Naya, S.-i.; Teranishi, M.; Aoki, R.; Tada, H. Fermi Level Control of Gold Nanoparticle by the Support: Activation of the Catalysis for Selective Aerobic Oxidation of Alcohols. *J. Phys. Chem. C* **2016**, *120*, 12440−12445.

(8) Ciriminna, R.; Scandura, G.; Pandarus, V.; Delisi, R.; Scurria, A.; Béland, F.; Palmisano, G.; Pagliaro, M. Towards the Broad Utilization of Gold Nanoparticles Entrapped in Organosilica. *ChemCatChem* **2017**, *9*, 1322−1328.

(9) Ciriminna, R.; Fidalgo, A.; Pandarus, V.; Béland, F.; Ilharco, L. M.; Pagliaro, M. New Catalyst Series from the Sol-Gel Entrapment of Gold Nanoparticles in Organically Modified Silica Matrices: Proof of Performance in a Model Oxidation Reaction. *ChemCatChem* **2015**, *7*, 254−260.

(10) Gregg, S. J.; Sing, K. S. *Adsorption, Surface Area and Porosity*, 2nd ed.; Academic Press: San Diego, 1982.

(11) Petkov, V.; Peng, Y.; Williams, G.; Huang, B.; Tomalia, D.; Ren, Y. Structure of Gold Nanoparticles Suspended in Water Studied by X-Ray Diffraction and Computer Simulations. *Phys. Rev. B: Condens. Matter Mater. Phys.* **2005**, *72*, 195402.

(12) Casaletto, M. P.; Longo, A.; Martorana, A.; Prestianni, A.; Venezia, A. M. XPS Study of Supported Gold Catalysts: the Role of Au^0 and Au$^{+\delta}$ Species as Active Sites. *Surf. Interface Anal.* **2006**, *38*, 215−218.

(13) Dimitratos, N.; Lopez-Sanchez, J. A.; Morgan, D.; Carley, A.; Prati, L.; Hutchings, G. J. Solvent Free Liquid Phase Oxidation of Benzyl Alcohol Using Au Supported Catalysts Prepared Using a Sol Immobilization Technique. *Catal. Today* **2007**, *122*, 317−324.

(14) Li, G.; Enache, D. I.; Edwards, J.; Carley, A. F.; Knight, D. W.; Hutchings, G. J. Solvent-Free Oxidation of Benzyl Alcohol with Oxygen Using Zeolite-Supported Au and Au-Pd Catalysts. *Catal. Lett.* **2006**, *110*, 7−13.

(15) Pagliaro, M.; Pandarus, V.; Béland, F.; Ciriminna, R.; Palmisano, G.; Demma Cara, P. A New Class of Heterogeneous Pd Catalysts for Synthetic Organic Chemistry. *Catal. Sci. Technol.* **2011**, *1*, 736−739.

(16) Pandarus, V.; Ciriminna, R.; Gingras, G.; Béland, F.; Pagliaro, M.; Kaliaguine, S. Hydrogenolysis of C-O Chemical Bonds of Broad Scope Mediated by a New Spherical Sol-Gel Catalyst. *ChemistryOpen* **2018**, *7*, 80−91.

(17) Ciriminna, R.; Pandarus, V.; Delisi, R.; Scurria, A.; Giordano, F.; Casaletto, M. P.; Béland, F.; Pagliaro, M. Sol-Gel Encapsulation of Au Nanoparticles in Hybrid Silica Improves Gold Oxidation Catalysis. *Chem. Cent. J.* **2016**, *10*, 61.

(18) Fidalgo, A.; Ciriminna, R.; Ilharco, L. M.; Pagliaro, M. Role of the Alkyl-Alkoxide Precursor on the Structure and Catalytic Properties of Hybrid Sol-Gel Catalysts. *Chem. Mater.* **2005**, *17*, 6686−6694.

(19) Avnir, D. Organic Chemistry within Ceramic Matrixes: Doped Sol-Gel Materials. *Acc. Chem. Res.* **1995**, *28*, 328−334.

(20) Brühne, F.; Wright, E. Benzaldehyde In *Ullmann's Encyclopedia of Industrial Chemistry*, Elvers, B., Ed.; Wiley-VCH: Weinheim, 2012; pp 223−235.

(21) Fan, J.; Dai, Y. H.; Li, Y. L.; Zheng, N. F.; Guo, J. F.; Yan, X. Q.; Stucky, G. D. Low-Temperature, Highly Selective, Gas-Phase Oxidation of Benzyl Alcohol over Mesoporous K-Cu-TiO$_2$ with Stable Copper(I) Oxidation State. *J. Am. Chem. Soc.* **2009**, *131*, 15568−15569.

(22) World Health Organization. Essential Medicines and Health Products, *WHO Model Prescribing Information: Drugs Used in Skin Diseases*; WHO: Geneva, 1997.

(23) Kesavan, L.; Tiruvalam, R.; Ab Rahim, M. H.; bin Saiman, M. I.; Enache, D. I.; Jenkins, R. L.; Dimitratos, N.; Lopez-Sanchez, J. A.; Taylor, S. H.; Knight, D. W.; Kiely, C. J.; Hutchings, G. J. Solvent-Free Oxidation of Primary Carbon-Hydrogen Bonds in Toluene Using Au-Pd Alloy Nanoparticles. *Science* **2011**, *331*, 195−199.

(24) Tanaka, K.; Toda, F. Solvent-Free Organic Synthesis. *Chem. Rev.* **2000**, *100*, 1025−1074.

(25) Ciriminna, R.; Pandarus, V.; Béland, F.; Pagliaro, M. Fine Chemical Synthesis Under Flow Using the Silia*Cat* Catalysts. *Catal. Sci. Technol.* **2016**, *6*, 4678−4685.